The effect of temperature on the mechanical properties and forming limit diagram of Al 5083 produced by equal channel angular rolling

J. Eisaabadi Bozcheloei, M. Sedighi, R. Hashemi*

School of Mechanical Engineering, Iran University of Science and Technology, Tehran, Iran

*Corresponding author:
e-mail: rhashemi@iust.ac.ir (R. Hashemi) Tel.: +98-21-77240068, Fax: +98-21-77240540

Abstract

The primary purpose of this research is investigating the effect of increasing temperature on mechanical properties and formability of Al 5083 produced by equal channel angular rolling (ECAR) process. The present work also aims to study the feasibility of increasing temperature as an approach for solving the ductility problem of ultrafine-grained Al 5083, although some strength of the material might be sacrificed. So, the quantitative and qualitative analysis of the effect of temperature increase on mechanical properties and formability has been done. In this paper, the ECAR process has been performed at three different temperatures (i.e., 25℃, 200℃, and 300℃). Then, the investigation of mechanical properties such as yield strength, ultimate tensile strength, and micro-hardness after each pass of the ECAR at different temperatures has been performed. The results showed that by applying the ECAR process at a specified temperature, the mechanical and micro-hardness properties of the samples improved, while elongation to fracture reduced. At ambient temperature, and after the 3rd pass of the ECAR process, yield strength, ultimate tensile strength, and micro-hardness compared to the annealed sample increased by 94%, 19%, and 52%, respectively. Also, the mechanical properties of samples after the ECAR process in a specified pass at different temperatures have been evaluated. The obtained results showed that by increasing temperature, the yield strength, ultimate tensile strength and micro-hardness of the samples decreased, but the elongation to fracture as well as the forming limit diagram (FLD) improved. The results illustrated that by applying the ECAR process at a specified temperature, the level of the FLDs moved downward. Also, the FLDs after the 3rd pass of the ECAR at different temperature have been compared. The results showed that the FLD_0 (the major forming limit strain in-plane strain mode) at a temperature of 200℃ and 300℃ compared to the ambient temperature increased by 5% and 20%, respectively.

Keywords
Equal channel angular rolling, Forming limit diagram, Temperature, Mechanical properties.

Introduction

Aluminum alloy 5083 uses further in the construction of pressure vessels, submarines, rocket components, and transportation equipment [1]. Recently, investigation of production methods and mechanical properties of materials with nanometer grain size or ultrafine-grained materials (UFG), has been the subject of many studies in the field of materials science [2]. The severe plastic deformation (SPD) process has been considered as one of the methods for producing materials with nanometer grain size [3, 4]. The equal channel angular rolling (ECAR) process is one of the methods of SPD [5]. ECAR is based on equal channel angular pressing (ECAP), which is carried out on large, thin sheets. In this process, thin metal sheets, without changing the dimensions, would be subjected to shear strain through the channels of a die set [6]. ECAR process has the capability for industrial applications. For example, ECAR can be combined with conform, to process ultrafine-grained materials continuously. So far, many materials have been produced using ECAR process, and mechanical properties, microstructure, residual stress, and texture have been investigated, including pure aluminum and its alloys [5-10], magnesium [11-15], and copper [16].

Hassani and Ketabchi [15] studied the influence of the number of ECAR passes on texture evolution of AZ31 magnesium alloy. They controlled ECAR temperature to prevent cracking along with maximizing the grain refinement efficiency. The initial average grain size of the as-received AZ31 sheet was about 21 μm. After 10 passes of the ECAR process, substantial grain refinement occurred, and the size of grains was reduced considerably to about 14–70 nm. Micro-hardness variation was investigated at ambient temperature. A continuous improvement of hardness was achieved by increasing the pass number of the process. The hardness values augmented by 53% at the 8th pass. At final passes, hardness decreased slightly due to the saturation of strain in the high number of passes.

Despite high strength to weight ratio in UFG metals produced by SPD methods, elongation decrease is a major problem [17-21]. Rahmatabadi and Hashemi [2] evaluated the mechanical properties and forming limit diagrams (FLDs) of ultrafine-grained aluminum strips fabricated by accumulative roll bonding (ARB) at room temperature. The specimens were well processed through ARB up to the 7th pass. The mechanical properties, crystallite size, and tensile fracture surfaces of specimens were examined. After the 7th pass, the amount of hardness, yield strength, and ultimate tensile strength raised by 106%, 408%, and 277% in comparison with the annealed sample, respectively. The ARB process leads to a substantial decrease in the elongation at break and major strain forming limit at plane strain condition (i.e., FLD_0), about 77.5% and 37%, respectively, up to the 7th pass. Also, Rahimi and his co-workers [5] investigated the mechanical properties and forming limit diagrams of ECARed Al 5083 sheets at ambient temperature and up to three passes. After the 3rd pass, the amount of hardness, yield strength, and ultimate tensile strength raised by 73%, 75%, and 14% in comparison with the annealed sample, respectively. The ECAR process leads to a substantial decrease in the elongation at break and major strain forming limit at plane strain condition (i.e., FLD_0), about 50% and 29%, respectively, up to the 3rd pass.

The results of research works showed that after ECAR process on various materials mechanical properties such as yield strength, ultimate tensile strength, and hardness had been improved (e.g., for in aluminum, copper, and steel). Also, after the ECAR process, elongation decreased for these materials.

However, no research has been done to investigate the effect of temperature on mechanical properties and forming limit diagram of ultrafine grained Al 5083 sheets. For the first time, the present work aims to examine the feasibility of increasing temperature as an approach for solving the ductility problem of ultrafine-grained metals, although the strength might be sacrificed. Also, the quantitative and qualitative analysis of the effect of temperature increase on mechanical properties and formability has been done. For this purpose, the ECAR process has been performed at ambient temperature, 200°C and 300°C up to 4, 5, and 7 passes on the samples, respectively. Then, the mechanical properties and forming limit diagrams of Al 5083 sheets fabricated by ECAR process at ambient temperature and high temperature (i.e., 200°C and 300°C) have been evaluated experimentally for the first time. By comparing the mechanical properties of samples after the ECAR process in a specified pass at different temperatures. We observed that by increasing temperature, the yield strength, ultimate tensile strength and micro-hardness of the samples decreased, but the elongation to fracture and forming limits were improved.

Experimental procedure

Material

In this research, the 5083 aluminum alloy has been used in the form of sheets of 2 mm in thickness. Initial samples (prototypes) have been prepared with the dimensions of $300 \times 60 \times 2$ mm^3 (length, width, thickness). The chemical composition of the aluminum alloy has been obtained using quantometery and X-ray fluorescence (XRF) analyses, as reported in Table 1. Before proceeding to the equal channel angular rolling process, the samples have been annealed to achieve a fully coaxial structure. The annealing process has been performed in a furnace at 450℃ for 1 hour according to the ASTM B918-01 standard procedure. Then, the annealed samples have been air-dried in the furnace.

Table 1. Chemical composition and mechanical properties of Al 5083 alloy.

Material	Chemical composition (wt. %)	Sample dimensions (l, w, t) (mm)	Hardness (HVN)	Yield strength (MPa)	Elongation (%)
Aluminum alloy 5083 annealed	Al, 4.47 Mg, 0.26 Fe, 0,089 Si, 0.049 Cu, 0.55 Mn, 0.057 Cr	300, 60, 2	78.2	146	9.1

Equal channel angular rolling process

Figure 1 presents a schematic of the ECAR process that has been used for shear deformation of metal sheets. The ECAR process has been practiced using a pair of rollers with a diameter of 121

mm, and two dies, namely an upper and a lower die. For this purpose, firstly, the dies have been attached to the body of the ECAR machine via some fixture. For each pass of the process, the upper die has been disassembled by unscrewing the respective nuts. Then, the samples have been taken out of the space between the two dies. The inlet and outlet channels had different thicknesses. The inlet channel thickness (the gap between the two rollers) was 1.90 mm and that of the outlet channel (the gap between faces of the dies) was 2 mm. Once the samples passed through the die, they retained their initial thickness (2 mm). The most significant angles in the ECAR process include an oblique angle (Φ) and curvature angle (Ψ). In the present research, zero curvature angle along with an oblique angle (which presents the angle of intersection between inlet and outlet channels) of 130° have been considered.
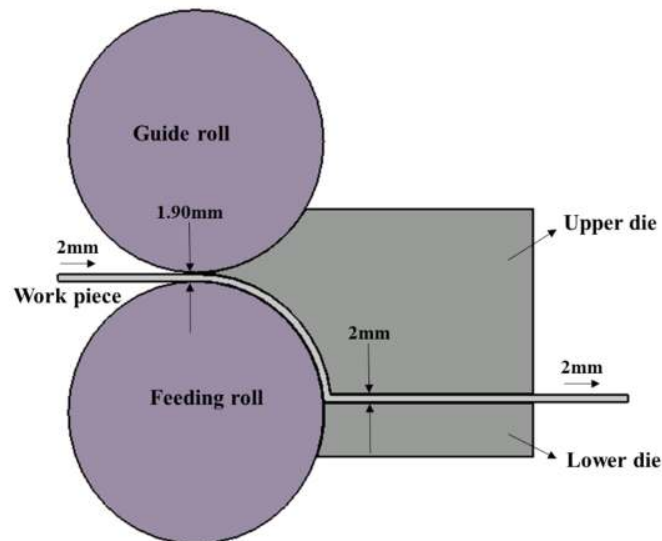

Figure 1. Schematic illustration of equal channel angular rolling (ECAR) process.

For the ECAR process paths, we adopted the same concepts as those used in the ECAP process. There would be four different paths in ECAP. In the ECAR process, one dimension of the sample (sheet thickness) is significantly smaller than the other dimensions. So, the process would be feasible only through the paths A and C. Along the path A, the sample remains without rotation, while it is rotated by 180° in either clockwise or counterclockwise direction along path C [22]. In this research, the ECAR process has been carried out on 5083 aluminum alloy at ambient temperature, 200℃, and 300℃. For this purpose, before each pass of the process, the samples have been preheated by a heater for 20 minutes. Then, the corresponding temperature measured by a thermocouple. The ECAR process has been performedat three different temperatures (25℃, 200±5℃, and 300±5℃).The samples have been injected into the die at 12-15 m/min. The high-temperature molybdenum disulfide (MoS2) has been used as a lubricant to reduce the friction between the sheet and die. Its operating temperature is up to 450℃ and friction coefficient is assumed 0.09. The samples have been fed into the die through the passing path C.

Depending on the material type and processing temperature, the number of passes a sample could be subjected to ECAR would be different. Then, some cracks could be observed on the sample surface following several passes of ECAR. Given the high strength of 5083 aluminum alloy, it could tolerate up to 4, 5, and 7 passes at ambient temperature, 200℃, and 300℃, respectively. At the fourth, fifth, and seventh pass at ambient temperature, 200℃, and 300℃, respectively, severe cracks have been developed on the sample due to the application of intensive work hardening to the specimen.

Mechanical properties

To study the mechanical properties of the samples, for each pass, two samples have been prepared for uniaxial tensile testing along the rolling direction (Figure 2). The samples have been made according to the ASTM E8/E8M-9 standard procedure through wire cutting. The uniaxial tensile tests have been performed at room temperature at a strain rate of 1×10^{-4} s^{-1} on a SANTAM-STM50 machine. Upon completing the uniaxial tensile test, stress-strain curves have been obtained for each pass.

Figure 2. The samples prepared for the uniaxial tensile test.

Vickers microhardness test was conducted to determine the hardness of the samples manufactured via the ECAR process. Performed on a JENUS machine under a load of 200 gr and a load application time of 10 s, the tests measured the microhardness along with the thickness of the sample. Before performing the microhardness test, the samples should be prepared. For this purpose, specimens with approximate dimensions of 2×1 cm have been cut out of the samples and placed into pre-cut plastic tubes. In order to make up the specimens with sandpaper, those should be mounted. Cold-mounting has been adopted for this purpose. Once the samples have been mounted, their surfaces have been polished by a rotating device equipped with sandpapers of different grits: 200, 400, 600, 800, 1200, and 1500. For each sample, the Vickers microhardness test has been performed at more than five random points. Then, omitting the outliers and averaging the remaining measurements, the microhardness of the specimen has been obtained.

Following the uniaxial tensile test, the cross-section of the fractured samples has been studied using a VEGA TESCAN scanning electron microscope (SEM). So, the fracture mechanism at different passes has been investigated.

Experimental determination of forming limit diagrams

The Nakazima test has been adopted to obtain forming limit diagrams (FLDs) [2, 23]. For this purpose, samples of various widths and a length of 200 mm have been cut from metal sheets in the rolling direction at ambient temperature, 200℃, and 300℃. Once the samples have been prepared, circular grids of 2.5 mm in diameter have been marked on the samples via electrochemical marking. A 50-ton constant speed hydraulic press (2 mm/min) has been used to draw the samples. A drop of force in a force-displacement diagram of the press could be presented as an occurrence of necking in a corresponding sheet.
Figure 3 presents the dimensions of the samples used to develop the FLDs [24]. Gridded and deformed samples following the Nakazima test can be observed in Figure 4. Following the Nakazima test on the gridded samples, forming limit strains of the samples have been determined by measuring principal and secondary strains of the ellipses within the closest distance to local crack zone (necking zone). Accordingly, a Mylar tape has been utilized for this purpose (Figure 5). For the sake of the measurements, the Mylar tape has been superimposed on the ellipse in such a way that its crossing lines were along the considered diameter. Then, the tape has been moved on the ellipse to have one of the lines equal to the considered diameter [23].
Using the Mylar tape, the major (d_1) and minor (d_2) diameters of the ellipse have been measured. Equations (1) and (2) have been used to measure major and minor strains:

$$\varepsilon_{major} = \ln(\frac{d_1}{d_0}) \tag{1}$$

$$\varepsilon_{minor} = \ln(\frac{d_2}{d_0}) \tag{2}$$

Where d_1, d_2, and d_0 are major and minor axes of the ellipse and the diameter of the initial circle, respectively. Upon calculating the major and minor strains for all of the samples of the FLD test, an intersection is obtained; passing a curve through these points, FLD can be obtained.
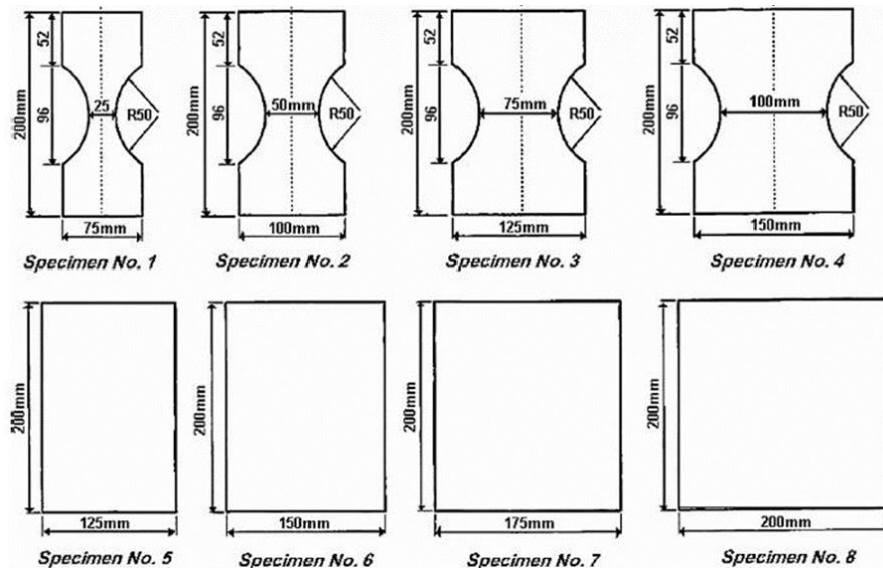
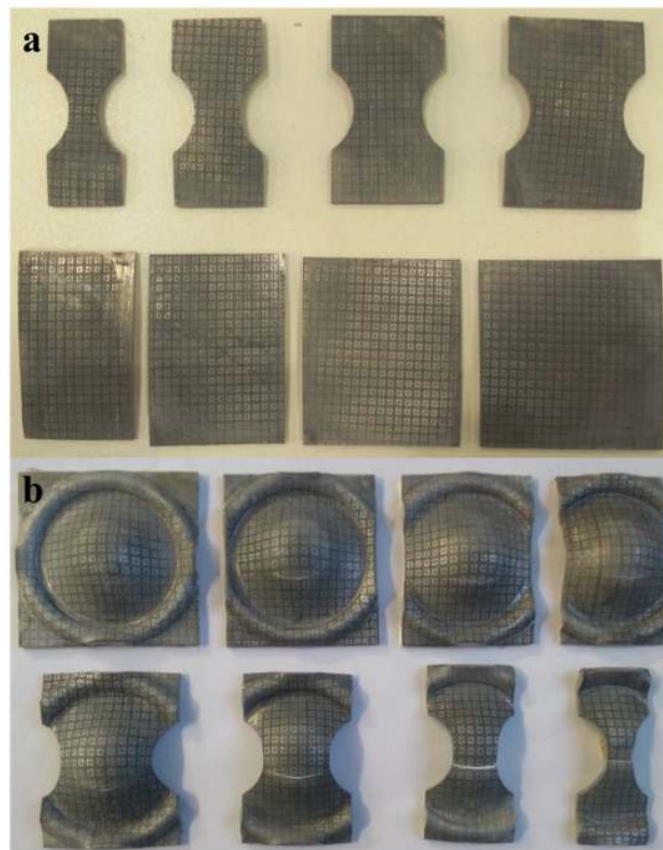**Figure 3.** Dimensions of standard samples for obtaining FLD [24].

Figure 4. (a) The gridded samples for FLD testing; (b) the samples after testing.
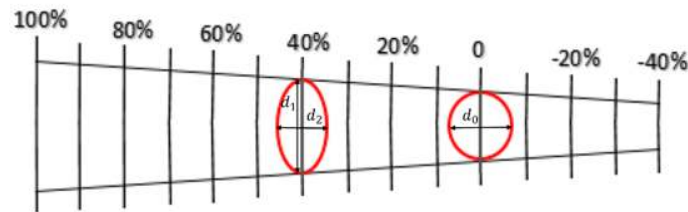
Figure 5. The Mylar transparent tape [5]

Results and discussion

Tensile properties

Figures 6 and 7 demonstrate true stress-strain curve and variations of yield strength, ultimate tensile strength, and elongation percentage of the processed samples of 5083 aluminum alloy versus passes of the process at ambient temperature, 200°C, and 300°C, along with those of the annealed samples, respectively. On these figures, it is evident that, with increasing the number of passes of the ECAR process, tensile strength increased while elongation decreased. Variations of tensile strength in metals subjected to sever plastic deformation could result from either of two root causes: work hardening by dislocations and grain refinement [25]. Because of the increased density of dislocations, strain hardening, application of large strains, and cold working. At the end of the first pass of the process, yield strength and ultimate tensile strength increased abruptly while the elongation percentage dropped sharply. The increase of the strength in subsequent passes of the process was primarily because of the grain structure evolution (microstructural modification) rather than the formation of fine grains. So, the rates at which yield strength increased and elongation decreased were significantly lower, as compared to those in the first pass [26-28]. In latter passes of the ECAR process, yield strength and ultimate tensile strength of the samples remained almost unchanged. In the latest pass, compared to the previous pass, the strain rate exhibited a slight decrease due to saturation of the density of dislocations and attenuation of the effect of strain hardening rate. This was because of the occurrence of recrystallization as materials reach stable-state density. The stable-state density was determined by establishing a dynamic balance between the development of dislocations during plastic deformation, and destruction of the dislocations during dynamic reversal processes which lower their microhardness slightly [16]. Figure 8 shows variations of yield strength and elongation percentage for different numbers of passes in the ECAR process at ambient temperature, 200°C, and 300°C for up to three such passes. As can be observed, at a given temperature, with increasing the number of passes, yield strength decreased while a higher elongation percentage was obtained. The decrease in yield strength along with the improved elongation percentage could result from one of the following reasons: (1) with increasing the temperature, effect of strain hardening was attenuated and hence density of dislocations decreased; (2) at elevated temperatures, the required amount of internal energy for triggering dynamic recovery or recrystallization would be generated, both of which contribute to the elimination of dislocations, thereby softening the material. The combined effect of the

recrystallization and dynamic recovery reduced the required stress for deformation. An increase in temperature reduced internal stresses and strength while increasing the elongation percentage [29, 30].
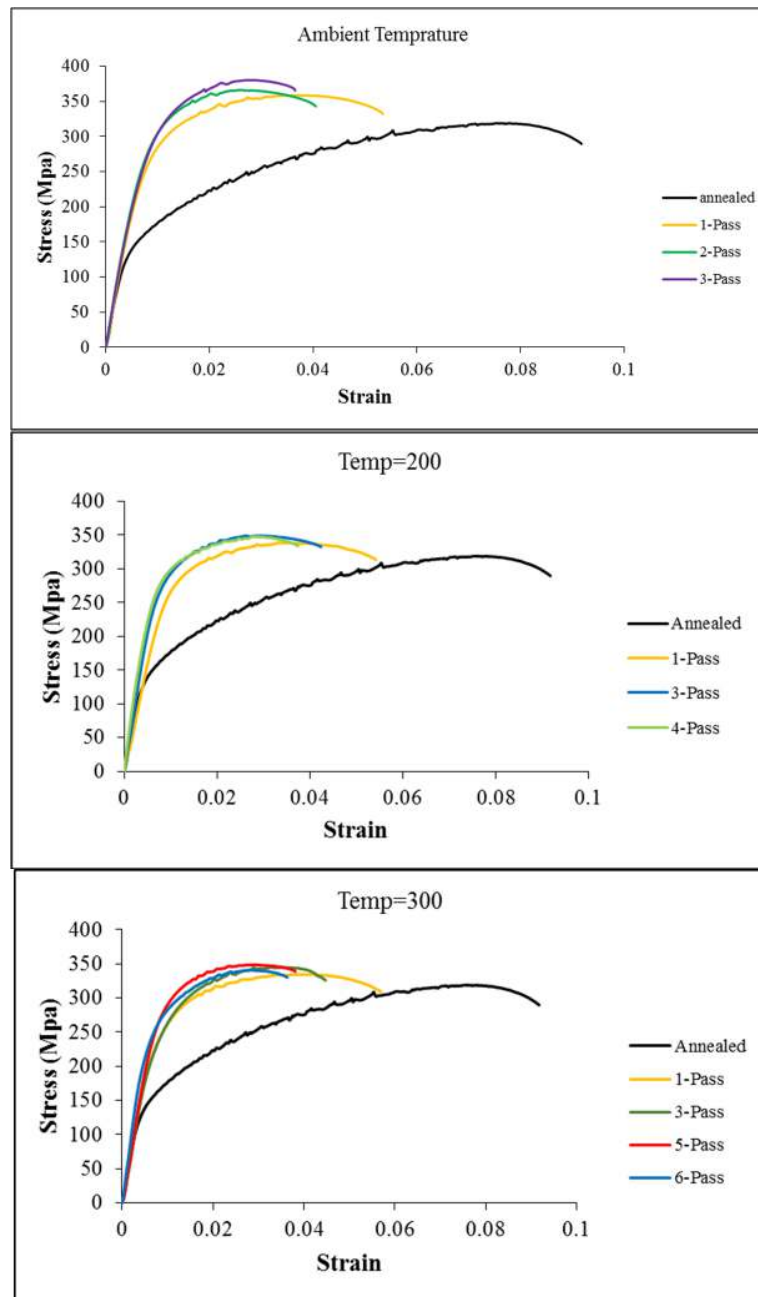

Figure 6. The true stress-strain curves for annealed samples and samples passed from ECAR die set at ambient temperature, 200℃, and 300℃.
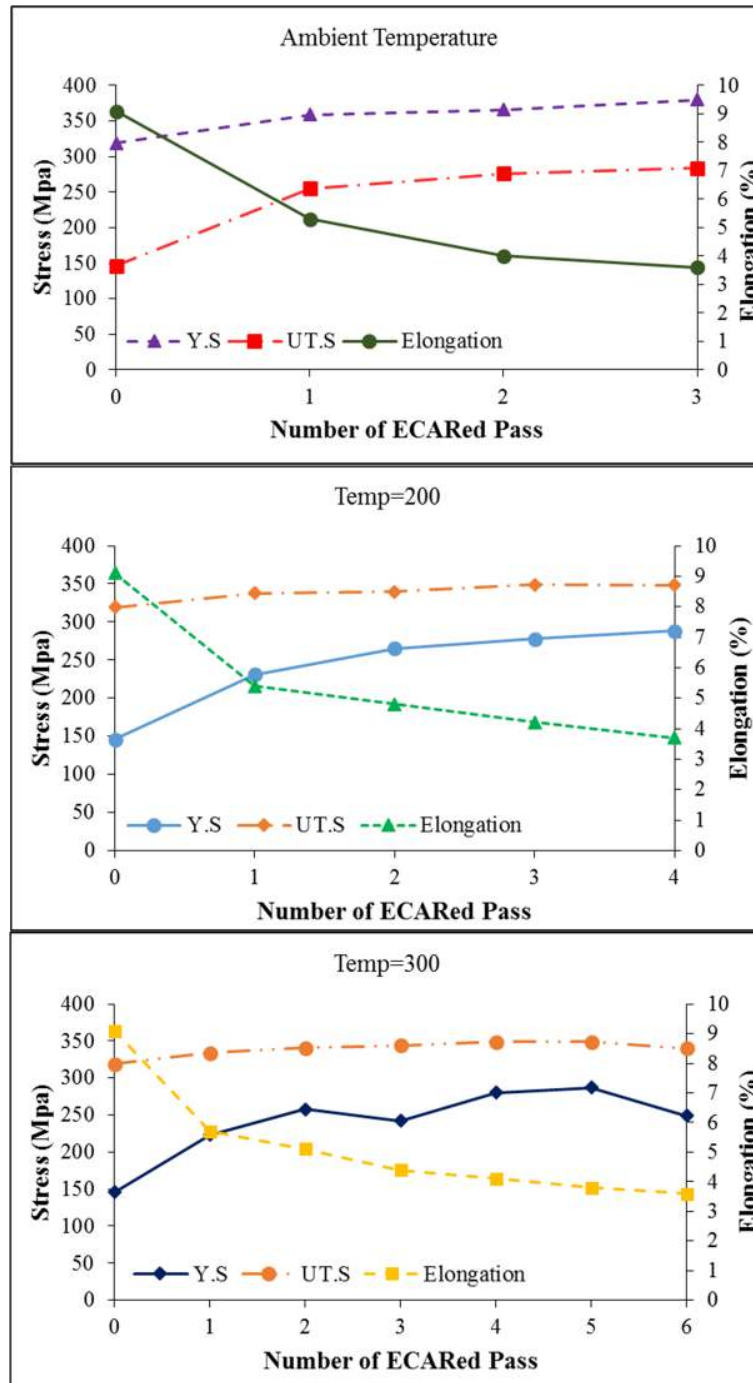
Figure 7. The variations of yield strength, ultimate tensile strength and elongation based on the number of ECARed passes at ambient temperature, 200℃, and 300℃.
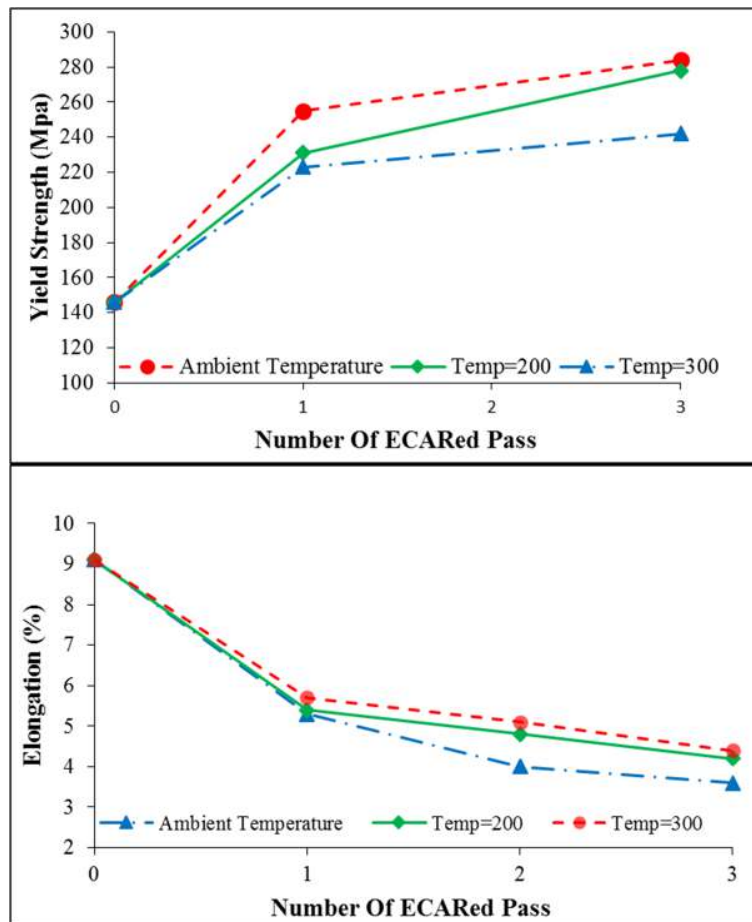
Figure 8. The variations of yield strength and elongation up to 3 passes of ECAR process at ambient temperature, 200℃, and 300℃.

The mechanical properties of different samples are given in Table 2.

Table 2. The mechanical properties of samples passed from ECAR die set at different temperature after the uniaxial tensile test.

Sample	Yield strength σ_y(Mpa)	Ultimate tensile strength (Mpa)σ_{UTS}	Elongation at break %El
Anneal	146	319	9.1
Pass 1 ECAR at Ambient Temperature	255	359	5.3
Pass 3 ECAR at Ambient Temperature	284	380	3.6
Pass 1 ECAR at 200℃	231	338	5.4
Pass 3 ECAR at 200℃	278	349	4.2
Pass 1 ECAR at 300℃	223	334	5.7
Pass 3 ECAR at 300℃	242	344	4.4

Microhardness

Figure 9 shows the variations of Vickers microhardness of the annealed samples as well as those passed through the die in the ECAP process in terms of the pass number at ambient temperature, 200°C, and 300°C. As can be observed, with increasing the number of passes, the microhardness of the samples increased. At the end of the first pass of the process, due to the increased density of dislocations because of strain hardening, microhardness increased at a steep slope [31]. Following the first pass, microhardness was seen to rise at some lower rate due to attenuation of the effect of strain hardening in subsequent passes.

Moreover, the microhardness remained almost the same at the latter passes at 200°C and 300°C due to the saturation of the density of dislocations and attenuation of the effect of strain hardening rate. At the final pass, crack development on the surface of the metal sheet decreased the sample hardness [32]. Figure 10 demonstrates Vickers microhardness values for the different number of passes of the sample through the die in ECAR process, where the results for up to 3 passes at ambient temperature, 200°C, and 300°C are shown. Comparing variations of microhardness for up to 3 passes at different temperatures, it can be seen that, in similar passes, the hardness increased slightly with increasing the temperature, due to the attenuated effect of strain hardening rate at elevated temperature. Besides, higher deformation temperature and lower strain rate are known to form coarser grains throughout the deformation stage, thereby lowering the resultant hardness [31].

Fractography of the samples

Fracture cross-sections of the annealed samples, as well as those passed through the die in ECAR for a different number of passes, were investigated using SEM following tensile testing. Dominant failure mechanism in the metals with the side-centered cubic crystal structure is cavity formation followed by soft failure [33]. In most cases, ductile fracturing occurs in the form of coaxial or hemispherical dimples [1, 2]. This type of failure occurred with the formation of micro-cavities, integration, crack propagation, and then shear failure along a direction close to that of tension (Figure 11) [27].
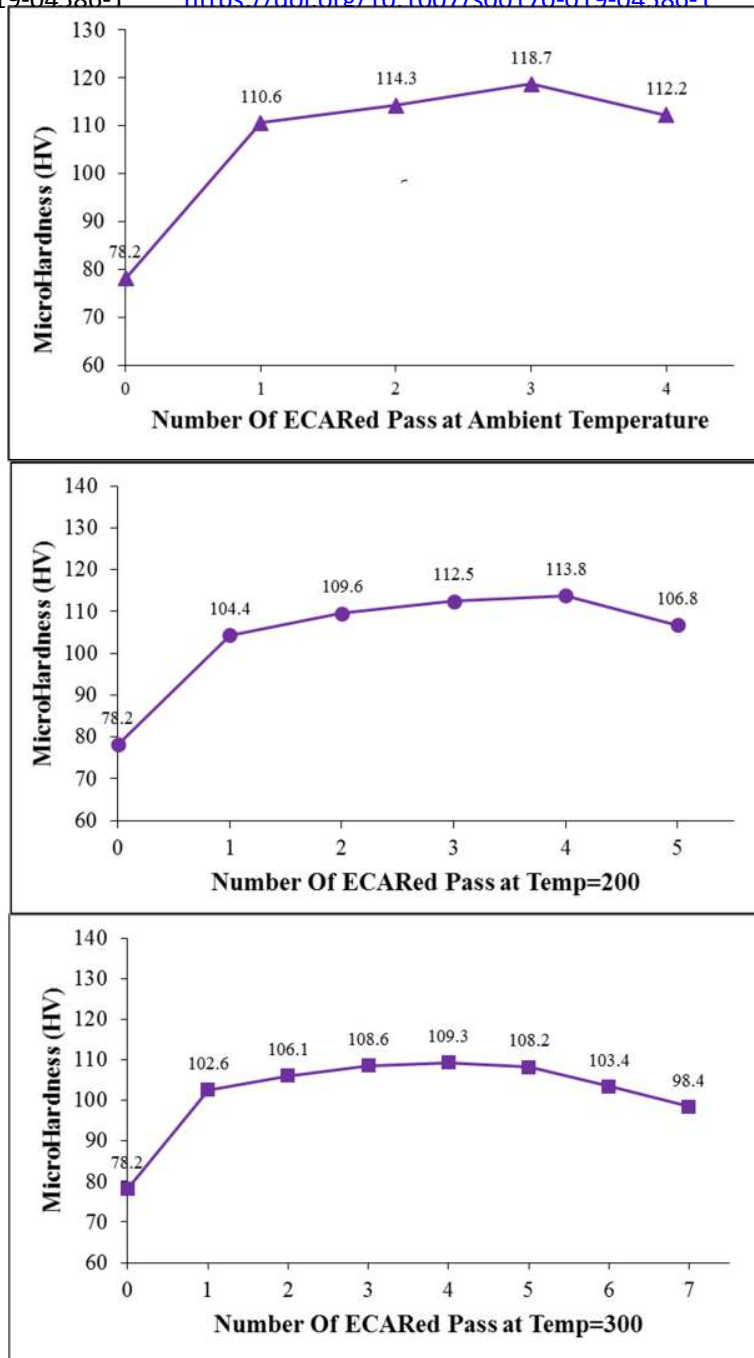
Figure 9. The variations of Vickers microhardness of the annealed samples as well as those passed through the die in the ECAP process in terms of the pass number at ambient temperature, 200°C, and 300°C.
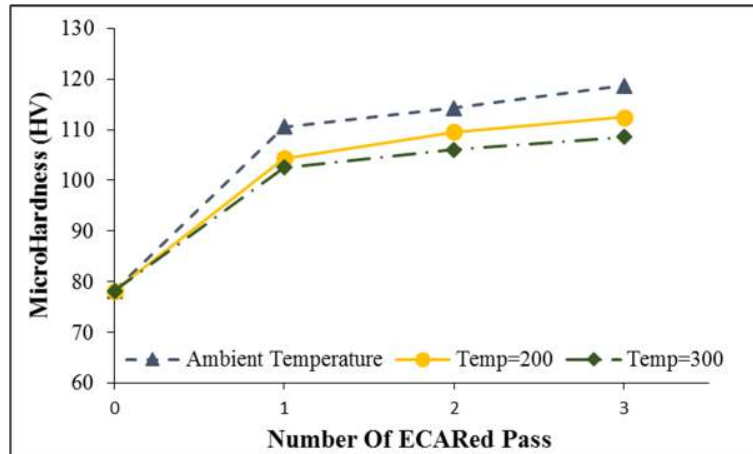
Figure 10. The variations of microhardness up to 3 passes of ECAR process at ambient temperature and also at 200℃ and 300℃.
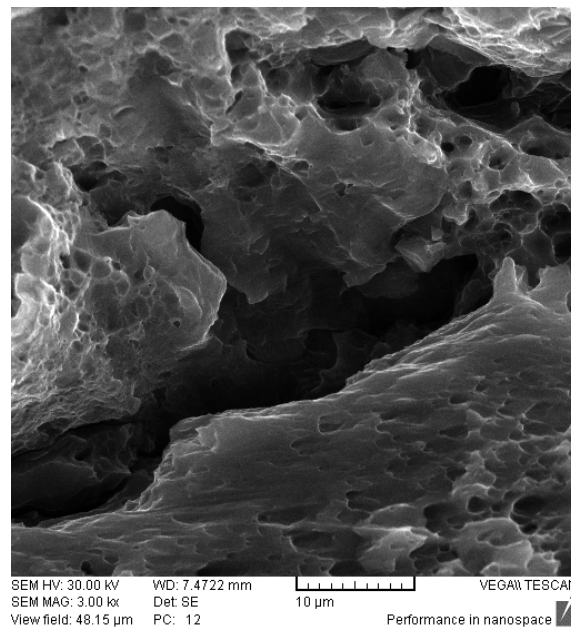

Figure 11. The tensile fracture surfaces of the sample after 3 passes the ECAR process at 300℃ .

Figure 12 demonstrates the fracture cross-section of the annealed sample as well as sample subjected to the ECAR process for one pass. Moreover, fracture cross-section of the samples passed through the die in the ECAR process at 300°C for different numbers of passes is shown in Figure 13. Based on the figures, with increasing the number of passes of the ECAR process, the micro-cavities got smaller and shallower compared to the annealed sample. The appearance of these micro-cavities in the rupture surfaces of the ECARed samples suggests the occurrence of the common shear ductile fracture mechanism similar to the initial sample, but micro-cavities get

smaller and shallower, causing increased tensile strength and decreased elongation compared to the initial sample.

The presence of shallower and smaller cavities was an indication of shear ductile fracturing which resembles the failure in the initial sample, with the only difference being the shallower depth of the fractures in this case. This could be interpreted as higher tensile strength, and hence, lower elongation percentage in the samples passed through the die, as compared to the initial (annealed) samples [34-38]. The failure surfaces of the initial and ECARed samples (Figure 12) show some hemispheroidal and micro-cavities, and that some micro-cavities are distributed in one or other direction because of applying unequal triaxial stresses. These dimples are features of a typical ductile fracture. Each micro-cavities is attributed to a crack nucleation site, which is linked up during the plastic deformation process [39].
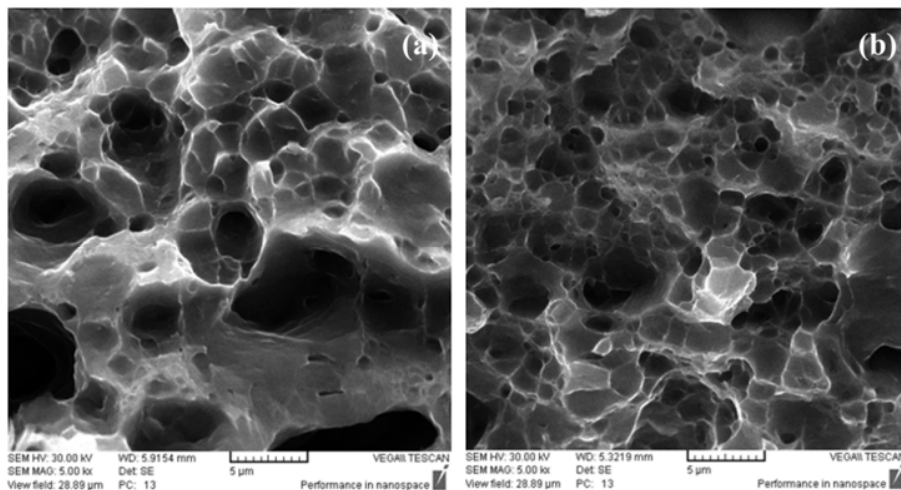

Figure12. The tensile fracture surfaces of (a) the initial sample and (b) after one pass of the ECAR process at ambient temperature.
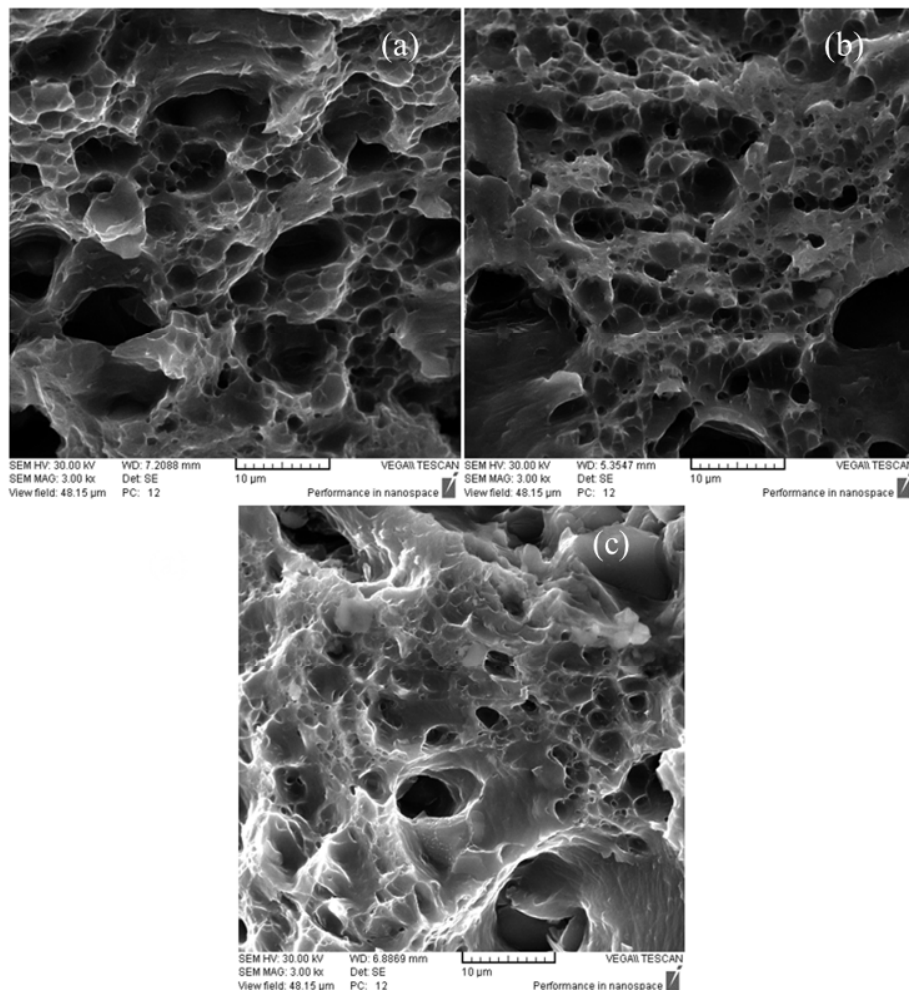
Figure13. The tensile fracture surfaces of (a) after one pass, (b) after three passes and (c) after five passes of the ECAR process at 300℃

Forming limit diagram of metal sheets

Figure 14 presents the FLDs obtained from experimentation on the annealed 5083 aluminum alloy samples and those subjected to ECAR in the first and third passes at ambient temperature. Comparing the obtained FLDs, one can conclude that, the area under the FLD curve of the samples subjected to the ECAR was much smaller than that of the annealed samples, indicating reduced formability following the ECAR process. The root cause of such a reduction was the high level of strain hardening in the first pass, which imposed the most significant contribution to lower FLDs. Due to the attenuated effects of work hardening and microstructural changes, the reduction in formability was lower in the third pass, as compared to the first pass. Comparing FLD_0 of each pass of the sample through the ECAR die to that of the annealed sample, some 28% and 48% decreases in formability were evident following the first and third passes, respectively [5]. Figures 15 and 16 show FLDs at different temperatures for the samples subjected to the ECAR in the first

and third passes, respectively. Comparing the corresponding FLDs to different temperatures, it is seen that, the formability improved slightly with increasing the temperature, because of the attenuated effect of work hardening at elevated temperatures and hence lower dislocation density which tended to add to elongation and consequently formability. Indeed, the decrease in dislocation density at high temperatures could be attributed to the occurrence of recrystallization and dynamic recovery during the ECAR process. Given that stacking fault energy (SFE) of the aluminum was high, the recovery processes performed faster [35]. Moreover, upon an increase in temperature, sufficient internal energy for initiation of the dynamic recovery or recrystallization was generated. The combined effect of the recrystallization and dynamic recovery reduced the required stress for deformation. An increase in temperature reduced the internal stresses and strength while increased the elongation percentage and formability [29].
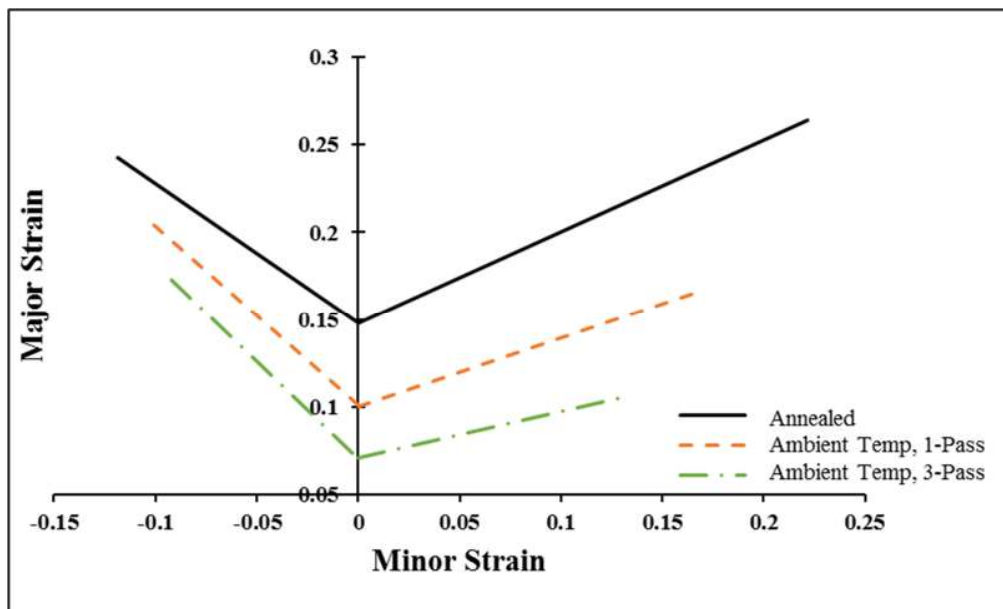

Figure14. The FLDs of annealed and first and third pass of ECARed aluminum 5083 at ambient temperature.
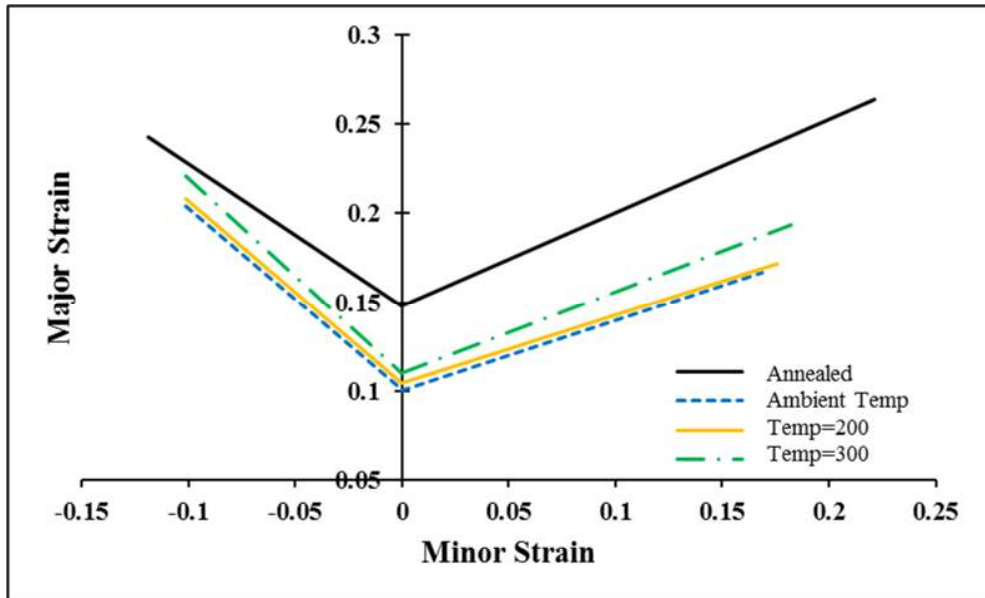
Figure15. The FLDs of annealed and first pass of ECARed aluminum 5083 at three different temperatures (ambient, 200℃ and 300℃).
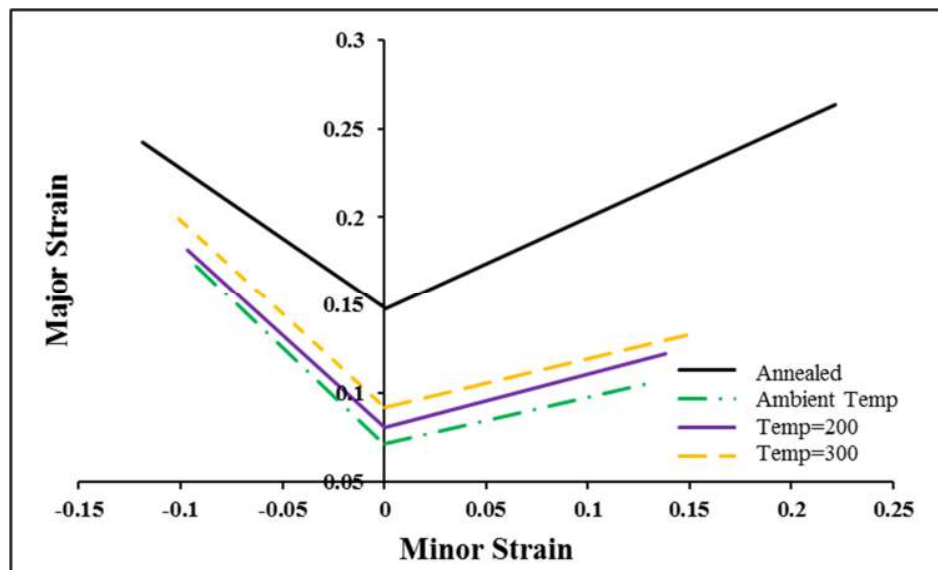
Figure16. The FLDs of annealed and third pass of ECARed aluminum 5083 at three different temperatures (ambient, 200℃ and 300℃).

Figure 17 compares the FLDs of the samples in different passes and at different temperatures. As can be observed, the ECAR process decreased the formability of the samples compared to those of the annealed samples. The results on the formability of the samples are introduced in Table 3. As indicated by the table, upon three passes of the ECAR at ambient temperature, elongation percentage and FLD_0 of the samples decreased by about 60% and 48%, respectively, as compared to the annealed sample. Moreover, following the third pass of ECAR at 300°C, elongation

percentage and FLD_0 of the samples decreased by 52% and 38%, respectively, as compared to the annealed sample. Comparing the results obtained for the samples subjected to three passes of the ECAR process at ambient temperature and 300°C, it was observed that the value of FLD_0 at 300°C was about 20% higher than that at ambient temperature.

Figure17. The FLDs of annealed, first and third pass of ECARed aluminum 5083 at three different temperatures (ambient, 200°C and 300°C).
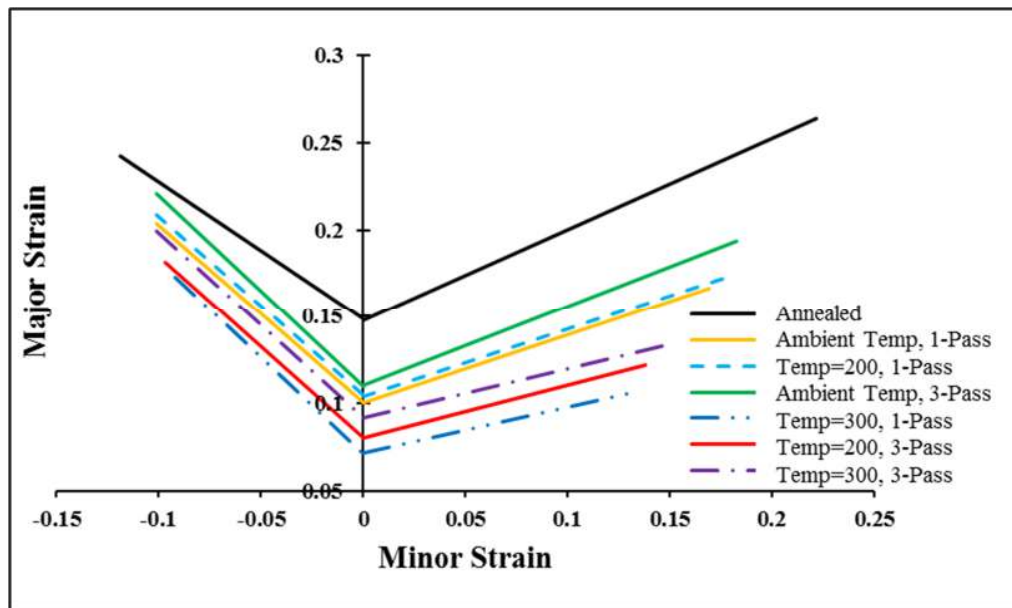
Table 3. The results of the formability aluminum 5083 at three different temperatures (Ambient, 200°C and 300°C).

Sample	Elongation at break (%El)	FLD_0	Percentage changes FLD_0 relative to the annealed sample	Percentage changes El relative to the annealed sample
Anneal	9.1	0.148	–	–
Pass 1 ECAR at Ambient Temperature	5.3	0.106	-28%	-42%
Pass 1 ECAR at 200°C	5.4	0.113	-23%	-40%
Pass 1 ECAR at 300°C	5.7	0.120	-19%	-37%
Pass 3 ECAR at Ambient Temperature	3.7	0.077	-48%	-60%
Pass 3 ECAR at 200°C	4.2	0.081	-45%	-54%
Pass 3 ECAR at 300°C	4.4	0.092	-38%	-52%

Conclusion

In this article, mechanical properties and forming limit diagrams of Al 5083 produced by equal channel angular rolling process were investigated at three different temperatures (ambient, 200°C, and 300°C), and the following results were obtained:

1- At ambient temperature, the continuous improvement was observed in yield strength and

ultimate tensile strength by applying three passes of the ECAR process. The maximum yield strength value and ultimate tensile strength were obtained after the third pass of the ECAR process, which was 284 MPa and 380 MPa, respectively. In comparison with the annealed samples, the yield strength and the ultimate tensile strength after the three passes of the ECAR process increased by 94% and 19%, respectively. Also, at ambient temperature, the elongation and FLD_0 values were decreased by increasing the number of the ECAR passes. After the 3-passes of the ECAR process compared to the annealed samples, registering 60% and 48% decreases, respectively.

2- By increasing the number of ECAR passes, the microhardness of the samples increased. At ambient temperature, microhardness was quickly enhanced after the 1st pass of the ECAR process, and then by increasing the ECAR process up to 3 passes, it was slowly enhanced. In the next passing due to created surface cracks, the microhardness was reduced slightly. The maximum hardness value was in the third pass of the ECAR process was 118.7 Vickers. That is a 52% increase, compared to the annealed samples.

3- By comparing the mechanical properties of samples after the ECAR process in a specified pass at different temperatures observed that by increasing temperature, the yield strength, ultimate tensile strength and microhardness values of the samples decreased. At the end of the third pass at 300°C, the yield strength, ultimate tensile strength and microhardness values of the samples in comparison with the ambient temperature decreased by 14.8%, 9.5%, and 8.5%, respectively.

4- By increasing the number of ECAR passes, at high temperatures (200 and 300°C), as the ambient temperature, forming limits reduced. By comparing forming limit diagram of the first and third pass at different temperatures, it was observed that in similar passes, the ductility value increased with increasing temperature in comparison with the ambient temperature. The FLD_0 values for the third pass, at the ambient temperature, 200°C and 300°C were obtained 0.077, 0.081, and 0.092, respectively. In other words, The FLD_0 values, at 200°C and 300°C in comparison with the ambient temperature increased by 5% and %20, respectively.

References

[1]   D. Rahmatabadi, R. Hashemi, B. Mohammadi, T. Shojaee, Experimental evaluation of the plane stress fracture toughness for ultra-fine grained aluminum specimens prepared by accumulative roll bonding process, Materials Science and Engineering: A, Vol. 708, pp. 301-310, 2017.

[2]   D. Rahmatabadi, R. Hashemi, Experimental evaluation of forming limit diagram and mechanical properties of nano/ultra-fine grained aluminum strips fabricated by accumulative roll bonding, International Journal of Materials Research, Vol. 108, No. 12, pp. 1036-1044, 2017.

[3]   M. Javidikia, R. Hashemi, Mechanical anisotropy in ultra-fine grained aluminium tubes processed by parallel-tubular-channel angular pressing, Materials Science and Technology, Vol. 33, No. 18, pp. 2265-2273, 2017.

[4]   D. Rahmatabadi, M. Tayyebi, R. Hashemi, G. Faraji, Microstructure and mechanical properties of Al/Cu/Mg laminated composite sheets produced by the ARB proces, International Journal of Minerals, Metallurgy, and Materials, Vol. 25, No. 5, pp. 564-572, 2018.

[5]   H. Rahimi, M. Sedighi, R. Hashemi, Forming limit diagrams of fine-grained Al 5083 produced by equal channel angular rolling process, Proceedings of the Institution of Mechanical Engineers, Part L: Journal of Materials: Design and Applications, Vol. 232, No. 11, pp. 922-930, 2018.

[6]   Y. H. Chung, J. woo Park, K. H. Lee, An analysis of accumulated deformation in the equal channel angular rolling (ECAR) process, Metals and Materials International, Vol. 12, No. 4, pp. 289, 2006.

[7]   J.-C. Lee, H.-K. Seok, J.-Y. Suh, Microstructural evolutions of the Al strip prepared by cold rolling and continuous equal channel angular pressing, Acta Materialia, Vol. 50, No. 16, pp. 4005-4019, 2002.

[8]   C. Nam, J. Han, Y. Chung, M. Shin, Effect of precipitates on microstructural evolution of 7050 Al alloy sheet during equal channel angular rolling, Materials Science and Engineering: A, Vol. 347, No. 1-2, pp. 253-257, 2003.

[9]   J.-H. Han, H.-K. Seok, Y.-H. Chung, M.-C. Shin, J.-C. Lee, Texture evolution of the strip cast 1050 Al alloy processed by continuous confined strip shearing and its formability evaluation, Materials Science and Engineering: A, Vol. 323, No. 1-2, pp. 342-347, 2002.

[10]   M. Mahmoodi, M. Sedighi, D. A. Tanner, Experimental study of process parameters' effect on surface residual stress magnitudes in equal channel angular rolled aluminium alloys, Proceedings of the Institution of Mechanical Engineers, Part B: Journal of Engineering Manufacture, Vol. 228, No. 12, pp. 1592-1598, 2014.

[11]   Y. Q. Cheng, Z. H. Chen, W. J. Xia, Drawability of AZ31 magnesium alloy sheet produced by equal channel angular rolling at room temperature, Materials characterization, Vol. 58, No. 7, pp. 617-622, 2007.

[12]   Y. Q. Cheng, Z. H. Chen, W. J. Xia, T. Zhou, Effect of channel clearance on crystal orientation development in AZ31 magnesium alloy sheet produced by equal channel angular rolling, Journal of materials processing technology, Vol. 184, No. 1-3, pp. 97-101, 2007.

[13]   Y. Q. Cheng, Z. H. Chen, W. J. Xia, Effect of crystal orientation on the ductility in AZ31 Mg alloy sheets produced by equal channel angular rolling, Journal of Materials Science, Vol. 42, No. 10, pp. 3552-3556, May 01, 2007.

[14]   Y. Q. Cheng, Z. H. Chen, W. J. Xia, T. Zhou, Improvement of drawability at room temperature in AZ31 magnesium alloy sheets processed by equal channel angular rolling, Journal of Materials Engineering and Performance, Vol. 17, No. 1, pp. 15-19, 2008.

[15]   F. Hassani, M. Ketabchi, Nano grained AZ31 alloy achieved by equal channel angular rolling process, Materials Science and Engineering: A, Vol. 528, No. 21, pp. 6426-6431, 2011.

[16]   A. Habibi, M. Ketabchi, M. Eskandarzadeh, Nano-grained pure copper with high-strength and high-conductivity produced by equal channel angular rolling process, Journal of Materials Processing Technology, Vol. 211, No. 6, pp. 1085-1090, 2011.

[17]   S.V. Noor, A.R. Eivani, H.R. Jafarian, M. Mirzaei, Inhomogeneity in microstructure and mechanical properties during twist extrusion, Materials Science and Engineering A, Vol. 652, pp. 186-191, 2016.

[18]   P. Teymoory, A. Zarei-Hanzaki, E. Farabi, H. Monajati, H.R. Abedi, Grain refinement through shear banding in severely plastic deformed A206 aluminum alloy, Advanced Engineering Materials, Vol. 20, No. 1, pp. 1700502, 2018.

[19]   F.J. Kalahroudi, A.R. Eivani, H.R. Jafarian, A. Amouri, R. Gholizadeh, Inhomogeneity in strain, microstructure and mechanical properties of AA1050 alloy during twist extrusion, Materials Science and Engineering: A, Vol. 667, pp. 349-357, 2016.

[20]   M.M. Mahdavian, H. Khatami-Hamedani, H.R. Abedi, Macrostructure evolution and mechanical properties of accumulative roll bonded Al/Cu/Sn multilayer composite, Journal of Alloys and Compounds, Vol. 703, pp. 605-613, 2017.

[21]   S. Valipour, A.R. Eivani, H.R. Jafarian, S.H. Seyedein, M.R. Aboutalebi, Effect of pre-deformation thermomechanical processing on the development of ultrafine grain structure during equal channel angular extrusion, Materials & Design, Vol. 89, pp. 377-384, 2016.

[22]   T. Naka, G. Torikai, R. Hino, F. Yoshida, The effects of temperature and forming speed on the forming limit diagram for type 5083 aluminum–magnesium alloy sheet, Journal of Materials Processing Technology, Vol. 113, No. 1-3, pp. 648-653, 2001.

[23]   R. Hashemi, G. Faraji, K. Abrinia, A. F. Dizaji, Application of the hydroforming strain-and stress-limit diagrams to predict necking in metal bellows forming process, The International Journal of Advanced Manufacturing Technology, Vol. 46, No. 5-8, pp. 551-561, 2010.

[24]   F. Ozturk, D. Lee, Experimental and numerical analysis of out-of-plane formability test, Journal of Materials Processing Technology, Vol. 170, No. 1, pp. 247-253, 2005.

[25]   M. Zhan, Y. Li, W. Chen, W. Chen, Microstructure and mechanical properties of Mg–Al–Zn alloy sheets severely deformed by accumulative roll-bonding, Journal of Materials Science, Vol. 42, No. 22, pp. 9256-9261, 2007.

[26]   Y. Saito, N. Tsuji, H. Utsunomiya, T. Sakai, R. Hong, Ultra-fine grained bulk aluminum produced by accumulative roll-bonding (ARB) process, Scripta materialia, Vol. 39, No. 9, pp. 1221-1227, 1998.

[27]   D. Rahmatabadi, B. Mohammadi, R. Hashemi, T. Shojaee, An Experimental Study of Fracture Toughness for Nano/Ultrafine Grained Al5052/Cu Multilayered Composite Processed by Accumulative Roll Bonding, Journal of Manufacturing Science and Engineering, Vol. 140, No. 10, pp. 101001-101001-11, 2018.

[28]   D. Rahmatabadi, M. Tayyebi, R. Hashemi, G. Faraji, Evaluation of Microstructure and Mechanical Properties of Multilayer Al5052–Cu Composite Produced by Accmulative Roll Bonding, Powder Metallurgy and Metal Ceramics, Vol. 57, No. 3, pp. 144-153, July 01, 2018.

[29]   H. McQueen, J. Jonas, Recovery and recrystallization during high temperature deformation, in: Treatise on Materials Science & Technology, Eds., pp. 393-493: Elsevier, 1975.

[30]   G. Rajaram, S. Kumaran, T. S. Rao, High temperature tensile and wear behaviour of aluminum silicon alloy, Materials Science and Engineering: A, Vol. 528, No. 1, pp. 247-253, 2010.

[31]   M. Shaarbaf, M. R. Toroghinejad, Nano-grained copper strip produced by accumulative roll bonding process, Materials Science and Engineering: A, Vol. 473, No. 1, pp. 28-33, 2008.

[32]   M. Alizadeh, M. Samiei, Fabrication of nanostructured Al/Cu/Mn metallic multilayer composites by accumulative roll bonding process and investigation of their mechanical properties, Materials & Design, Vol. 56, pp. 680-684, 2014.

[33]   D. Rahmatabadi, M. Tayyebi, A. Sheikhi, R. Hashemi, Fracture toughness investigation of Al1050/Cu/MgAZ31ZB multi-layered composite produced by accumulative roll bonding process, Materials Science and Engineering: A, Vol. 734, pp. 427-436, 2018/09/12/, 2018.

[34]   M. Naseri, A. Hassani, M. Tajally, Fabrication and characterization of hybrid composite strips with homogeneously dispersed ceramic particles by severe plastic deformation, Ceramics International, Vol. 41, No. 3, Part A, pp. 3952-3960, 2015.

[35]   F. J. Humphreys, M. Hatherly, Recrystallization and related annealing phenomena: Elsevier, 2012.

[36]   M. Sedighi, M. Mahmoodi, Residual stresses evaluation in equal channel angular rolled Al 5083 by IHD technique: Investigation of two calculation methods, Materials and Manufacturing Processes, Vol. 28, Issue 1, pp. 85-90, 2012.

[37]   M. Mahmoodi, M. Sedighi, D. A. Tanner, Investigation of through thickness residual stress distribution in equal channel angular rolled Al 5083 alloy by layer removal technique and X-ray diffraction, Materials & Design, Vol. 40, pp. 516-520, 2012.

[38]   H. Hakimian, M. Sedighi, A. Asgari, Experimental and numerical study on the ECARed magnesium AZ31 alloy, Mechanics & Industry, Vol. 17, Issue 1, pp. 110-116, 2016.

[39]   M. Reihanian, F.K. Hadadian, M.H. Paydar, Fabrication of Al–2 vol% Al2O3/SiC hybrid composite via accumulative roll bonding (ARB): an investigation of the microstructure and mechanical properties, Materials Science and Engineering: A, Vol. 607, pp. 188-196, 2014.